Molecular Microbiology (2011) 79(4), 929–939 ■
doi:10.1111/j.1365-2958.2010.07497.x
First published online 22 December 2010

SAP1 is a critical post-transcriptional regulator of infectivity in malaria parasite sporozoite stages

Ahmed S. I. Aly,[1†] Scott E. Lindner,[1] Drew C. MacKellar,[1] Xinxia Peng[1] and Stefan H. I. Kappe[1,2*]
[1]*Seattle Biomedical Research Institute, Seattle, WA 98109, USA.*
[2]*Department of Global Health, University of Washington, Seattle, WA 98195, USA.*

Summary

Plasmodium **salivary gland sporozoites upregulate expression of a unique subset of genes, collectively called the** ***UIS*** **(upregulated in infectious sporozoites). Many** ***UIS*** **were shown to be essential for early liver stage development, although little is known about their regulation. We previously identified a conserved sporozoite-specific protein, SAP1, which has an essential role in** ***Plasmodium*** **liver infection. Targeted deletion of** ***SAP1*** **in** ***Plasmodium yoelii*** **caused the depletion of a number of selectively tested** ***UIS*** **transcripts in sporozoites, resulting in a complete early liver stage arrest. Here, we use a global gene expression survey to more comprehensively identify transcripts that are affected by** ***SAP1*** **deletion. We find an effect upon both the transcript abundance of** ***UIS*** **genes, as well as of select genes previously not grouped as** ***UIS*****. Importantly, we show that the lack of SAP1 causes the specific degradation of these transcripts. Collectively, our data suggest that SAP1 is involved in a selective post-transcriptional mechanism to regulate the abundance of transcripts critical to the infectivity of sporozoites. Although** ***Pysap1***$^{-}$ **sporozoites are depleted of many of these important transcripts, they confer long-lasting sterile protection against wild-type sporozoite challenge in mice.** ***SAP1*** **is therefore an appealing candidate locus for attenuation of** ***Plasmodium falciparum*****.**

Accepted 1 December, 2010. *For correspondence. E-mail stefan.kappe@seattlebiomed.org; Tel. (+1) 206 256 7205; Fax (+1) 206 256 7229. †Present address: College of Medicine, King Saud Bin Abdulaziz University for Health Sciences, Jeddah 21423, Saudi Arabia.

Introduction

The malaria parasites' pre-erythrocytic stages (sporozoites and liver stages) are excellent targets for intervention strategies that attempt to prevent malaria because of their low numbers early in infection and their clinical silence within the human host (Aly *et al.*, 2009; Kappe *et al.*, 2010). Sporozoites form within oocysts on the mosquito midgut (Aly *et al.*, 2009). After egress into the haemolymph, sporozoites invade the salivary glands. Inside the salivary gland ducts, sporozoites can wait for several days before being transmitted during the next blood meal. After inoculation into the host's dermis, sporozoites enter the blood stream, migrate to the liver and infect hepatocytes, wherein they each transform into a liver stage and initiate exoerythrocytic schizogony. It remains largely unknown which molecular mechanisms control salivary gland sporozoite infectivity.

Sporozoites attenuated through genetic manipulation can be rendered unable to replicate in the liver and confer sterile protection against challenge in malaria mouse models (van Dijk *et al.*, 2005; Mueller *et al.*, 2005a,b; Labaied *et al.*, 2007; Tarun *et al.*, 2007; Aly *et al.*, 2008). Interestingly, the majority of successful loci targeted by genetic attenuation are of the upregulated in infectious sporozoites *(UIS)* group (Vaughan *et al.*, 2010). *UIS* genes were initially identified in a subtractive cDNA hybridization assay, and more recently through a comparative microarray analysis of liver-infectious and non-infectious sporozoites (Matuschewski *et al.*, 2002; Mikolajczak *et al.*, 2008). However, additional candidate proteins essential for liver stage development need to be identified to broaden our understanding of liver stage biology and to expand the repertoire of targets for genetic attenuation (Kappe *et al.*, 2010). To achieve this, a more thorough understanding of the regulation of sporozoite infectivity is also needed.

In a previous study, we showed that SAP1 (sporozoite asparagine-rich protein 1) is essential for early liver stage development of the parasite (Aly *et al.*, 2008). SAP1 localized to the cytoplasm of salivary gland sporozoites and deletion of SAP1 caused a reduction in transcript abundance of a subset of sporozoite-expressed genes (Aly *et al.*, 2008). This lead us to hypothesize that SAP1 is involved in a post-transcriptional mechanism of gene

expression regulation. However, another study analysing the orthologue of SAP1 in *Plasmodium berghei* (called SLARP: sporozoite and liver stage asparagine-rich protein) showed a nuclear localization (Silvie *et al*., 2008), indicative of a transcriptional regulatory function for SAP1.

Here, we further demonstrate that SAP1 does not localize to the nucleus but to the cytoplasm of *P. yoelii* sporozoites. Using microarray gene expression analysis, we find that many *UIS* transcripts are reduced because of the lack of SAP1. We also observed an additional set of non-*UIS* transcripts that are similarly regulated. Importantly, we show that the absence of SAP1 causes the terminal degradation of these transcripts, but not of other sporozoite transcripts. Our data consistently reveal that SAP1 is a key post-transcriptional regulator of transcripts critical to early liver stage infection.

Results

The abundance of UIS *and a set of non-*UIS *gene transcripts are significantly affected in* P. yoelii sap1$^-$ *sporozoites*

We previously established that *P. yoelii sap1*$^-$ (*Pysap1*$^-$) salivary gland sporozoites display a severe reduction in the transcript abundance of five tested *UIS* genes, whereas other sporozoite-expressed transcript levels such as those for circumsporozoite protein (CSP) and thrombospondin-related anonymous protein (TRAP) were unaffected (Aly *et al*., 2008). To investigate the genome-wide impact of the *SAP1* knockout on transcript expression, we screened for all transcripts that are downregulated in *Pysap1*$^-$ sporozoites using an oligonucleotide microarray that was designed based on the annotated open reading frames (ORFs) of the rodent malaria parasite *P. yoelii* (Carlton *et al*., 2002). The complete microarray data set can be accessed from the NCBI GEO database (Accession GSE12397).

To identify genes that are differentially expressed between *Pysap1*$^-$ and wild-type sporozoites, we used a non-parametric method based on the analysis of rank product. This procedure is expected to perform well when only a small number of biological replicates are available (Hong *et al*., 2006). We identified 38 genes, which were $\geq$ twofold downregulated, and 14 genes, which were $\geq$ twofold upregulated, when comparing *Pysap1*$^-$ and wild-type sporozoites (Fig. 1A and B). Among the downregulated genes were *UIS1, UIS2, UIS4*, *UIS7*, *UIS13, UIS16, UIS28* and *TLP* (TRAP-like protein), which were all identified as *UIS* genes in our previous microarray analysis (Mikolajczak *et al*., 2008) (Fig. 1A). Additional *UIS* transcripts (e.g. UIS3) were also identified using a less stringent 1.5-fold cut-off (Fig. S1). Interestingly, transcript abundance for a subset of genes that were not previously identified as *UIS* was also significantly regulated. Transcripts that were downregulated include those that encode for proteins predicted to bind RNA (PY02798) or DNA (PY02160, PY01408), along with others that putatively have specific enzymatic functions (e.g. transporters, kinases, methyltransferases; See Fig. 1). Additionally, the abundance of several transcripts was significantly increased, among which include RNA-binding proteins (PY03866, PY02598), a putative multi-drug efflux pump (PY04044) and predicted components of the general transcription machinery (PY01022, PY01352). Included in both groups were several proteins that could affect transcript stability and/or translation, including orthologues of RNA-binding proteins, such as Puf2 (PY04369) (Fig. 1). SAP1 might therefore regulate the normal balance of these factors to help produce its overall post-transcriptional effect.

In order to validate our data in terms of which subsets of genes are most affected in *Pysap1*$^-$ sporozoites, we also compared the current microarray results with our previously conducted *UIS-UOS* microarray analysis (Mikolajczak *et al*., 2008). A scatter plot analysis confirmed that the genes that were mostly upregulated in infectious sporozoites are also mostly downregulated in *Pysap1*$^-$ sporozoites (Fig. 2).

SAP1 localizes to the sporozoite cytoplasm

To substantiate the cytoplasmic subcellular localization of SAP1 that was first shown in our previous study by antisera against the C-terminus of SAP1 (Aly *et al*., 2008), we generated rabbit polyclonal antisera against the N-terminus of PySAP1. The need to confirm the cytoplasmic localization of SAP1 in *P. yoelii* arose because of conflicting data from another study that indicated that the SAP1 orthologue in *P. berghei* localized to the nucleus of salivary gland sporozoites (Silvie *et al*., 2008). We tested the antisera in immunofluorescence assays using *Pysap1*$^-$ and wild-type sporozoites. A consistent and specific staining pattern within the wild-type sporozoites was observed that excluded the nucleus and was distinct from CSP (Fig. 3A). The pattern of SAP1 presented with a strongly speckled, non-homogeneous distribution, indicative of localization to structures within the sporozoite cytoplasm, reminiscent of stress granules (Buchan *et al*., 2008). Pre-immune sera did not show any reactivity with wild-type sporozoites (data not shown). The staining pattern observed by the use of antibodies raised against the SAP1 N-terminal domain was similar to the localization data obtained with C-terminus-specific antisera (Aly *et al*., 2008). The specificity of the antisera against the N-terminal domain was confirmed by the lack of staining in *Pysap1*$^-$ sporozoites (Fig. 3B). The current findings thus confirm our previous observations that SAP1 localizes to the cytoplasm of *P. yoelii* sporozoites, likely trafficking to intracellular structures found within.

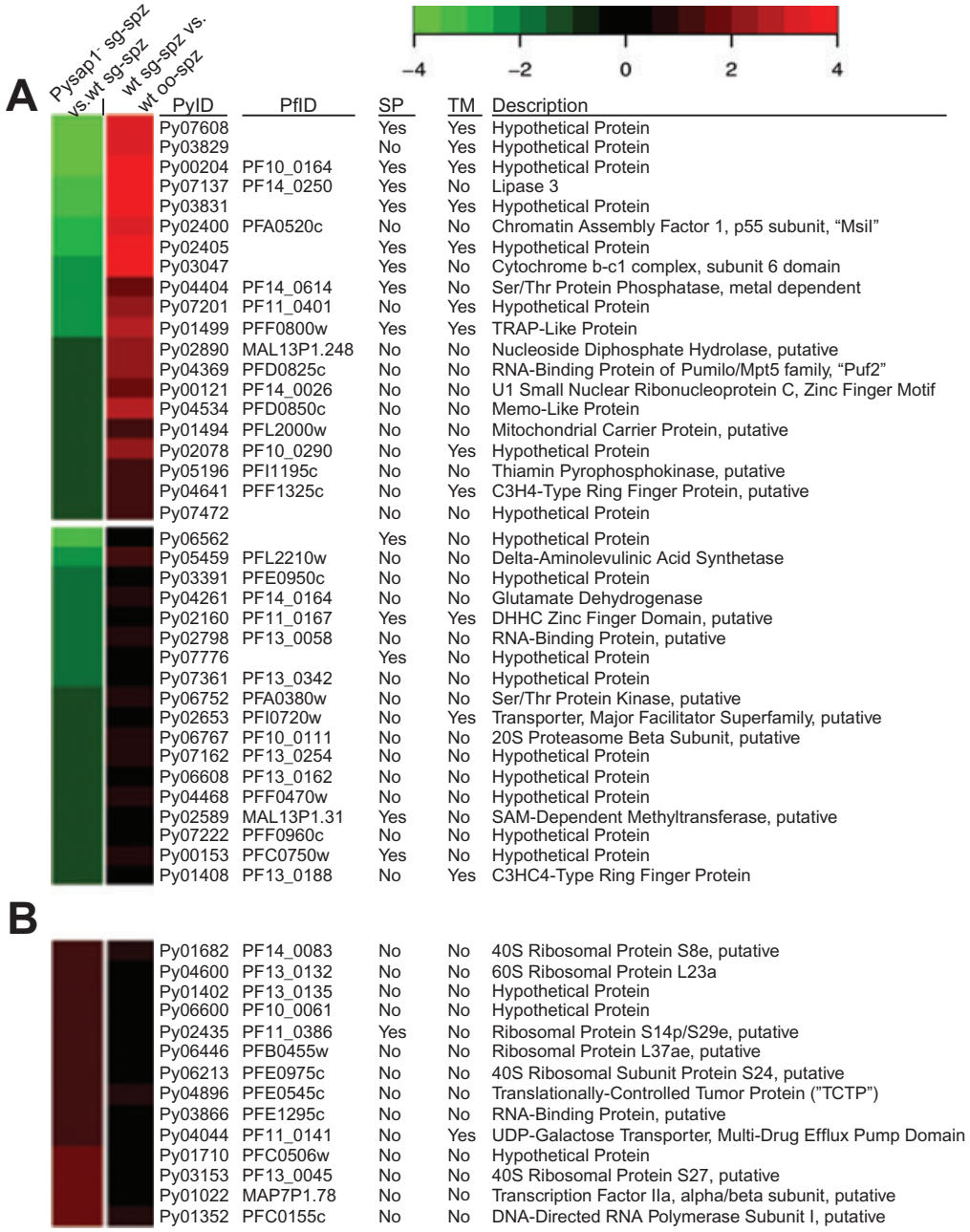

PyID	PfID	SP	TM	Description
Py07608		Yes	Yes	Hypothetical Protein
Py03829		No	Yes	Hypothetical Protein
Py00204	PF10_0164	Yes	Yes	Hypothetical Protein
Py07137	PF14_0250	Yes	No	Lipase 3
Py03831		Yes	Yes	Hypothetical Protein
Py02400	PFA0520c	No	No	Chromatin Assembly Factor 1, p55 subunit, "Msil"
Py02405		Yes	Yes	Hypothetical Protein
Py03047		Yes	No	Cytochrome b-c1 complex, subunit 6 domain
Py04404	PF14_0614	Yes	No	Ser/Thr Protein Phosphatase, metal dependent
Py07201	PF11_0401	No	Yes	Hypothetical Protein
Py01499	PFF0800w	Yes	Yes	TRAP-Like Protein
Py02890	MAL13P1.248	No	No	Nucleoside Diphosphate Hydrolase, putative
Py04369	PFD0825c	No	No	RNA-Binding Protein of Pumilo/Mpt5 family, "Puf2"
Py00121	PF14_0026	No	No	U1 Small Nuclear Ribonucleoprotein C, Zinc Finger Motif
Py04534	PFD0850c	No	No	Memo-Like Protein
Py01494	PFL2000w	No	No	Mitochondrial Carrier Protein, putative
Py02078	PF10_0290	No	Yes	Hypothetical Protein
Py05196	PFI1195c	No	No	Thiamin Pyrophosphokinase, putative
Py04641	PFF1325c	No	Yes	C3H4-Type Ring Finger Protein, putative
Py07472		No	No	Hypothetical Protein
Py06562		Yes	No	Hypothetical Protein
Py05459	PFL2210w	No	No	Delta-Aminolevulinic Acid Synthetase
Py03391	PFE0950c	No	No	Hypothetical Protein
Py04261	PF14_0164	No	No	Glutamate Dehydrogenase
Py02160	PF11_0167	Yes	Yes	DHHC Zinc Finger Domain, putative
Py02798	PF13_0058	No	No	RNA-Binding Protein, putative
Py07776		Yes	No	Hypothetical Protein
Py07361	PF13_0342	No	No	Hypothetical Protein
Py06752	PFA0380w	No	No	Ser/Thr Protein Kinase, putative
Py02653	PFI0720w	No	Yes	Transporter, Major Facilitator Superfamily, putative
Py06767	PF10_0111	No	No	20S Proteasome Beta Subunit, putative
Py07162	PF13_0254	No	No	Hypothetical Protein
Py06608	PF13_0162	No	No	Hypothetical Protein
Py04468	PFF0470w	No	No	Hypothetical Protein
Py02589	MAL13P1.31	Yes	No	SAM-Dependent Methyltransferase, putative
Py07222	PFF0960c	No	No	Hypothetical Protein
Py00153	PFC0750w	Yes	No	Hypothetical Protein
Py01408	PF13_0188	No	Yes	C3HC4-Type Ring Finger Protein

PyID	PfID	SP	TM	Description
Py01682	PF14_0083	No	No	40S Ribosomal Protein S8e, putative
Py04600	PF13_0132	No	No	60S Ribosomal Protein L23a
Py01402	PF13_0135	No	No	Hypothetical Protein
Py06600	PF10_0061	No	No	Hypothetical Protein
Py02435	PF11_0386	Yes	No	Ribosomal Protein S14p/S29e, putative
Py06446	PFB0455w	No	No	Ribosomal Protein L37ae, putative
Py06213	PFE0975c	No	No	40S Ribosomal Subunit Protein S24, putative
Py04896	PFE0545c	No	No	Translationally-Controlled Tumor Protein ("TCTP")
Py03866	PFE1295c	No	No	RNA-Binding Protein, putative
Py04044	PF11_0141	No	Yes	UDP-Galactose Transporter, Multi-Drug Efflux Pump Domain
Py01710	PFC0506w	No	No	Hypothetical Protein
Py03153	PF13_0045	No	No	40S Ribosomal Protein S27, putative
Py01022	MAP7P1.78	No	No	Transcription Factor IIa, alpha/beta subunit, putative
Py01352	PFC0155c	No	No	DNA-Directed RNA Polymerase Subunit I, putative

Fig. 1. Gene expression analysis reveals transcripts that are downregulated or upregulated in *Pysap1*⁻ salivary gland sporozoites when compared with wild-type salivary gland sporozoites.
A. The heat map shows the gene transcripts that are less abundant in *Pysap1*⁻ sporozoites in comparison with wild-type sporozoites. A set of 38 gene transcripts (first column) was identified as ≥ 2× less abundant in *Pysap1*⁻ sporozoites when compared with wild-type sporozoites (*Pysap1*⁻ sg-spz vs. wt sg-spz). The less abundant gene transcripts in *Pysap1*⁻ sporozoites were then compared with the *UIS* genes heat map (second column), which refers to genes differentially upregulated in salivary gland sporozoites compared with oocyst sporozoites (wt sg-spz vs. wt oo-spz).
B. The heat map shows the gene transcripts that are more abundant in *Pysap1*⁻ sporozoites in comparison with wild-type sporozoites. A set of 14 gene transcripts (first column) was identified as ≥ 2× more abundant in *Pysap1*⁻ sporozoites when compared with wild-type sporozoites [*sap1*(-)sg vs. WTsg]. Upregulated genes show no correlation to *UIS* gene expression (second column). In each heat map, the replicated hybridizations are shown as the mean for four replicates (two biological replicates and dye swaps of each biological replicate). Differentially expressed genes were selected using a rank-based algorithm with a false-discovery rate of 5%. The complete microarray data set can be accessed from the NCBI GEO database (Accession GSE12397).
PyID, *P. yoelii* gene identifier; PfID, *P. falciparum* gene identifier; SP, signal peptide; TM, transmembrane domain.

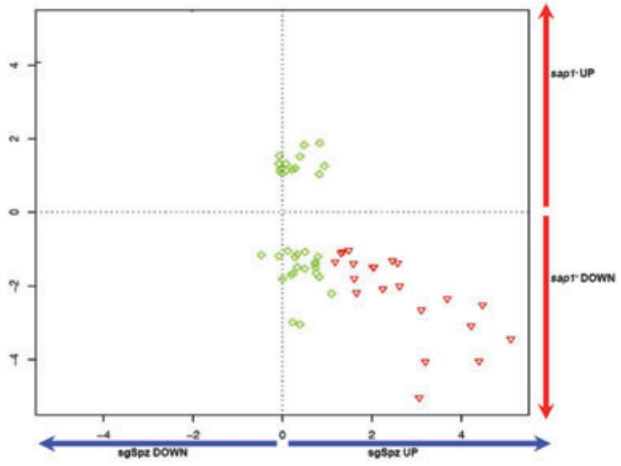

Fig. 2. The less abundant transcripts in *Pysap1*⁻ salivary gland sporozoites are mostly *UIS* genes. Differentially abundant transcripts from the *Pysap1*⁻ sporozoite vs. wild-type sporozoite expression analysis were aligned against the wild-type salivary gland sporozoite versus wild-type oocyst sporozoites (WTsg vs. WToo) expression analysis to identify the effect of *SAP1* deletion on transcript abundance of sporozoite genes. Inverted triangles represent *UIS* transcripts that are less abundant in *Pysap1*⁻ sporozoites. Diamonds represent transcripts that are less or more abundant in *Pysap1*⁻ sporozoites than wild-type sporozoites, but that are not defined as *UIS* genes.

To further resolve the discrepancies between our previous and current observations in *P. yoelii*, and those of Silvie and colleagues, who determined that the *P. berghei* orthologue of SAP1 fused to the fluorescent mCherry protein resided in the parasite nucleus and not in the cytoplasm (Silvie *et al.*, 2008), we fused mCherry to the C-terminus of PySAP1. Transgenic parasites in which the functional copy of SAP1 was replaced with one expressing a C-terminal mCherry tag were able to appropriately transcribe and splice the complete mRNA as determined by RT-PCR and subsequent sequencing of the products (Fig. S2). However, we were unable to observe the translated fusion protein either by live fluorescence microscopy or by immunofluorescence assay in any parasite life cycle stage (data not shown). Moreover, the transgenic sporozoites had the same phenotype as the *Pysap1*⁻ sporozoites: they were unable to induce a blood stage infection when inoculated into mice (Table S1). Taken together, the fusion of mCherry to the C-terminus of PySAP1 disrupts its function, perhaps by prohibiting its translation or adversely affecting the fusion protein's stability and is thus not an appropriate tool to determine SAP1's localization.

Degradation of the 3′ end of UIS *and non-*UIS *transcripts in* Pysap1⁻ *sporozoites*

The regulation of transcript abundance of a specific subset of genes could be due to a transcriptional or post-transcriptional mechanism. Transcriptional regulation of gene expression occurs almost exclusively within the nucleus, whereas post-transcriptional gene expression regulation is mostly executed in the cytoplasm (Balagopal and Parker, 2009; Buchan and Parker, 2009). The fact that SAP1 resides in the cytoplasm, or structures within the cytoplasm, implies that SAP1 could function in a post-transcriptional pathway of gene expression regulation. We hypothesized that SAP1 is involved in stabilizing a specific subset of transcripts in sporozoites inside the salivary glands. To test this hypothesis, we determined if the 5′ and 3′ termini of transcripts found to be downregulated in our microarray analysis were shortened or degraded in *Pysap1*⁻ sporozoites. We primarily chose to use 3′ RACE (rapid amplification of cDNA ends) to test for the occurrence of 3′ mRNA decay. In agreement with our hypothesis, we find that PCR products for the 3′ RACE test amplicons of these transcripts were only amplified from wild-type sporozoites and not from *Pysap1*⁻ sporozoites (Fig. 4B). We also used 3′ RACE to test the abundance of two non-*UIS* transcripts that were upregulated in *Pysap1*⁻ sporozoites, and observed a significant increase in transcript abundance for both (Fig. 4B). No amplicons were

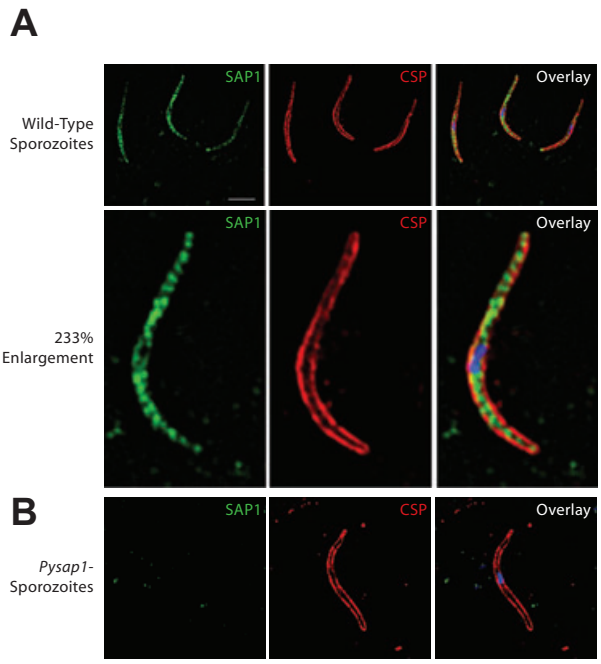

Fig. 3. SAP1 is localized to granular structures in the cytoplasm of *P. yoelii* sporozoites. Immunofluorescence assay of wild-type (A) or *Pysap1*⁻ (B) sporozoites using antisera generated against the N-terminus of SAP1. An internal localization of SAP1 is observed in wild-type sporozoites, but not in *Pysap1*⁻ sporozoites, demonstrating specificity of the antisera. The centre-most wild-type sporozoite is enlarged 233% to highlight the granular/speckled-staining pattern of SAP1, indicative of a localization to stress granules. Note the absence of SAP1 staining in the nucleus of wild-type sporozoites. DAPI was used to stain the nucleus of the sporozoite and CSP was used to visualize the sporozoite surface. Scale bar is 5 μm.

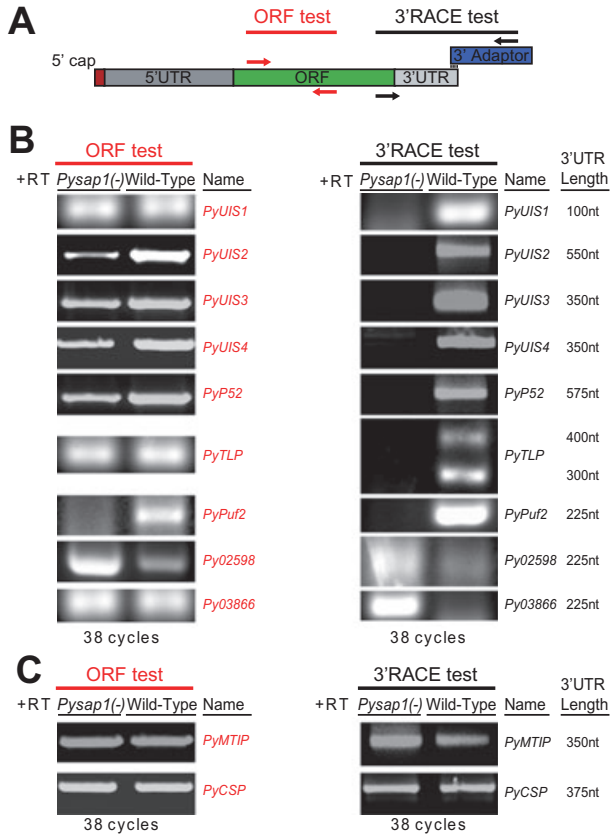

Fig. 4. 3′ RACE analysis shows 3′ mRNA degradation of *UIS* and some non-*UIS* transcripts.
A. A schematic of a mRNA molecule adapted for 3′ RACE. 3′ RACE and ORF primers and test amplicons are indicated.
B. 3′ RACE was conducted on RNA isolated from wild-type or *Pysap1*⁻ sporozoites that was reverse transcribed into cDNA with an oligo dT attached to a downstream DNA adaptor. The oligo dT binds only to non-degraded 3′ poly (A) mRNA species before reverse transcription to first strand cDNA (RT). PCR amplification using several independent gene-specific sense primers and a 3′ adaptor anti-sense primer resulted in specific amplicons with abundances consistent with the observations from the microarray experiment. Internal ORF amplicons could be produced from RNA of both parasite types.
C. *PyCSP* and *PyMTIP* 3′ RACE tests were used as positive controls for the 3′ RACE test amplification from *Pysap1*⁻ sporozoites. The approximate length of 3′UTRs from the stop codon is listed in 25 nt increments.

produced from RNA samples that were not treated with reverse transcriptase (data not shown). In contrast, we amplified 3′ RACE test amplicons for the non-*UIS* transcripts CSP and MTIP (Myosin-A Tail domain Interacting Protein) as positive controls from both sporozoite populations, and observed no significant difference in transcript abundance (Fig. 4C). However, it could be argued that the 3′ RACE test amplicon could not be amplified because of a severe reduction in the transcription of *UIS* genes caused by *SAP1* deletion. In order to address this concern, we used gene specific primers to the ORF of the transcripts under investigation. We were able to amplify ORF test amplicons for most of these transcripts from cDNA generated from *Pysap1*⁻ sporozoites, albeit mostly at lower abundance when compared with transcripts amplified from wild-type sporozoites (Fig. 4B). The reduced overall transcript abundance is likely due to complete degradation of a significant proportion of these transcripts, which can as a consequence no longer serve as a template for reverse transcription.

Degradation of the 5′ end of a representative UIS *transcript in* Pysap1⁻ *sporozoites*

We predicted that degraded transcripts would not have a 5′ cap structure, which protects the mRNA from exonucleases (Balagopal and Parker, 2009). We used the RLM-RACE (RNA ligase mediated rapid amplification of cDNA ends) technique to differentiate between capped and uncapped transcripts (Fig. 5A). We indeed find that the 5′ RACE test amplicon for the *UIS4* transcript was only amplified from wild-type sporozoites and not from *Pysap1*⁻ sporozoites (Fig. 5B). No amplicons were produced from RNA samples that were not treated with reverse transcriptase (data not shown). As a positive control, we amplified a 5′ RACE test amplicon for *CSP* equally from both sporozoite populations (Fig. 5B). We also tested 5′ RACE-processed RNA from both sporozoite populations in which no TAP treatment was carried out (–TAP) to serve as a negative control. Transcripts lacking the TAP treatment would retain their 5′ cap and would prevent the covalent attachment of the 5′RNA Adaptor. As expected, the 5′ RACE test amplicons for *UIS4* and *CSP* were not amplified from (–TAP) 5′ RACE-processed RNA from wild-type or *Pysap1*⁻ sporozoites (Fig. 5B). Similar to the 3′ RACE analysis, PCR products from the ORFs of *UIS4* and *CSP* were amplified from all 5′ RACE-processed RNAs for wild-type and *Pysap1*⁻ sporozoites. This demonstrates that the *UIS4* transcript and possibly other *UIS* transcripts additionally undergo 5′ degradation in *Pysap1*⁻ sporozoites.

Pysap1⁻ *sporozoites are a protective, long-lasting genetically attenuated vaccine*

Previous studies showed that immunization of BALB/c mice with three intravenous (iv) doses of 10 000 *Pysap1*⁻ sporozoites conferred sterile protection against wild-type sporozoite challenge (Aly *et al.*, 2008). The wild-type challenge was conducted either 30 days post-immunization (pi) by intravenous (iv) injection, or 45 days pi by mosquito bite. Groups of *Pysap1*⁻ immunized mice were re-challenged 180 days after the first wild-type sporozoite challenge, and were also found to be protected against wild-type sporozoites delivered either iv or by mosquito bite (Aly *et al.*, 2008). Importantly, in these re-challenge

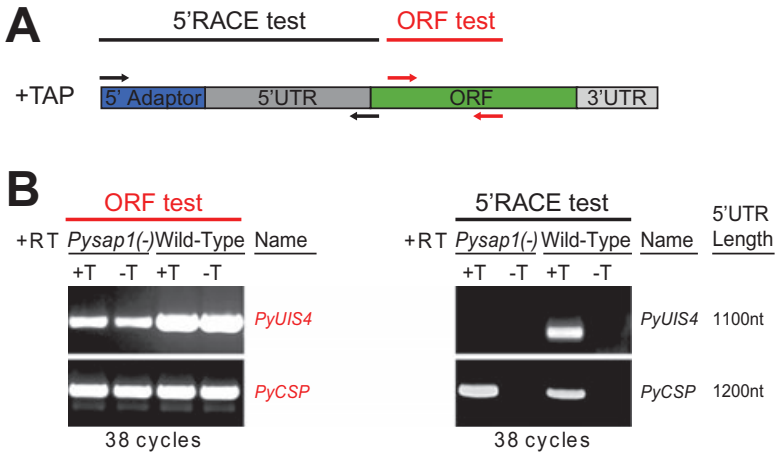

Fig. 5. 5′ RACE analysis shows 5′ mRNA degradation of a representative *UIS* transcript.
A. A schematic of an mRNA molecule adapted for 5′RACE. 5′RACE and ORF primers and test amplicons are indicated.
B. 5′ RLM-RACE analysis from RNA isolated from wild-type or *Pysap1*⁻ sporozoites that was treated with Tobacco acid Pyrophophatase (TAP) enzyme (+T) to remove the 5′ cap in undegraded mRNA species or not treated (–T). A 5′ RNA adaptor will only bind to TAP-treated (+T) (previously capped) mRNA species before reverse transcription into first strand cDNA. PCR Amplification using a 5′ adaptor sense primer and a *UIS4* 5′UTR anti-sense primer resulted in a specific amplicon only from wild-type sporozoites, while an *UIS4* internal ORF amplicon could be amplified from both types of sporozoites. *PyCSP* 5′ RACE test amplicons were used as positive controls for the experiment from both wild-type and *Pysap1*⁻ sporozoites.

experiments, the first challenge after 30 days provides a boosting dose. Conversely, data from another group utilizing immunizations done in C57BL/6 mice with *P. berghei sap1*⁻ sporozoites showed that protection is lost after 3 months pi (Silvie *et al*., 2008). In order to study the long-lasting protection in the *P. yoelii*/BALB/c model system, we tested groups of BALB/c mice that were immunized 3 times, in 2 week intervals, with 10 000 *Pysap1*⁻ sporozoites and first challenged iv 3 months, 6 months or 9 months pi with 10 000 *P. yoelii* wild-type sporozoites (Table 1). All immunized mice were completely protected against the challenges. Moreover, groups of BALB/c mice receiving three subcutaneous (sc) immunizations with 100 000 *Pysap1*⁻ sporozoites, three iv immunizations with 1000 *Pysap1*⁻ sporozoites or two iv immunizations with 50 000 *Pysap1*⁻ sporozoites were completely protected against wild-type sporozoite challenge 2 months, 3 months or 2 months after the final immunization respectively (Table 1). Furthermore, immunization of outbred Swiss Webster mice with 20 000 *Pysap1*⁻ sporozoites given four times, showed complete sterile protection (Table 1) against a first challenge 3 months after the last immunization. Finally, 1 year pi challenge by mosquito bite in BALB/c mice that were immunized 4 times with 10 000 *Pysap1*⁻ sporozoites demonstrated complete sterile protection. Collectively, these results show that immunizations with *Pysap1*⁻ salivary gland sporozoites confer sterile, protracted protection in Balb/c mice but also in outbred mice, which are more difficult to protect.

Table 1. Immunizations with *Pysap1*⁻ sporozoites confer long-lasting sterile protection against wild-type sporozoite challenge.

Mouse strain	Primary dose	Boosts (interval in days)	Challenge dose (months after last immunization)	Protected/ Challenged[a]
BALB/c	10 000	10 000 (14)/10 000 (28)	10 000 (3)	8/8
BALB/c	10 000	10 000 (14)/10 000 (28)	10 000 (6)	7/7
BALB/c	10 000	10 000 (14)/10 000 (28)	10 000 (9)	6/6
BALB/c	100 000 subq[b]	100 000 subq[b] (14)/100 000 subq[b] (28)	10 000 (2)	5/5
BALB/c	1 000	1 000 (14)/1 000 (28)	10 000 (3)	5/5
BALB/c	10 000	10 000 (14)/10 000 (28)/10 000 (42)	Mosquito bite[c] (12)	5/5
SW	20 000	20 000 (14)/20 000 (28)/20 000 (42)	20 000 (3)	5/5
BALB/c	50 000	50 000 (14)	10 000 (2)	5/5

All immunization and challenge sporozoite doses were administered to mice by intravenous injection, unless otherwise stated.
a. Each immunization group had an age-matched naïve parallel group of three mice, which all became blood stage patent at day 3 after wild-type sporozoite challenge.
b. Sporozoites were inoculated into mice by dorsal subcutaneous injection.
c. Infection through mosquito bite by allowing at least 20 wild-type-infected mosquitoes to bite each mouse for at least 15 min.

Discussion

In this study we demonstrate that *Pysap1*⁻ sporozoites undergo degradation of numerous transcripts that are normally upregulated when wild-type sporozoites gain infectivity for the mammalian host. Moreover, the 5′ and 3′ degradation patterns of these transcripts are comparable with mRNA decay mechanisms found in other eukaryotes. We observed that SAP1 also affects the transcript abundance of a small set of non-*UIS* genes both positively and negatively. A simple model to explain these observations places SAP1 as an essential part of mRNP (messenger ribonucleoprotein) complexes (termed stress granules) in salivary gland sporozoites, which selectively harbour and protect upregulated transcripts. In support of this, SAP1 localized to the cytoplasm of sporozoites in a speckled pattern, typical for stress granules. In a likely scenario, when SAP1 is deleted, stress granule assembly is severely affected and unprotected transcripts, which are no longer translationally repressed, would be instead directed into mRNA degradation pathways. The increase of the abundance of some transcripts in *Pysap1*⁻ sporozoites is certainly interesting as well, but may result from more complex, and possibly indirect effects of SAP1 deletion.

Several of the SAP1-regulated transcripts encode RNA-binding proteins, including the previously described *Plasmodium* Puf2 orthologue (Miao *et al*., 2010). In their study, Miao and colleagues observed that PfPuf2 affects the gametocyte sex ratio from the early stages of gametocytogenesis. This regulatory effect may be accomplished through the binding of PfPuf2 to one or more of the 95 mRNAs with predicted Puf-binding sites (Le Roch *et al*., 2004). Our findings indicate that Puf2 might have an additional and important function in sporozoites. Taken together, RNA-binding proteins such as those regulated by SAP1 could in turn directly bind to downstream mRNA targets to modulate their stability, and thus provide an additional means of post-transcriptional regulation in sporozoites. SAP1's regulation of Puf2 mRNA and mRNAs of other related proteins might therefore provide a central regulatory mechanism for transcript stability in sporozoites, which clearly warrants further investigation.

Post-transcriptional regulation of gene expression by translational repression of mRNAs is a sophisticated mechanism employed by most eukaryotic organisms (Beckham and Parker, 2008; Anderson and Kedersha, 2009; Balagopal and Parker, 2009; Buchan and Parker, 2009). It has been suggested that post-transcriptional regulation also plays a major role in gene expression control in *Plasmodium* (Shock *et al*., 2007). Interestingly, *Plasmodium* female gametocytes translationally repress a number of transcripts that are only needed after transformation into gametes and fertilization in the mosquito midgut (Mair *et al*., 2006). The DEAD-box RNA helicase, termed DOZI (development of zygote inhibited), was shown to be essential for translational repression, and null mutants of *DOZI* generated zygotes that were not able to proceed in their development (Mair *et al*., 2006). In metazoans, DEAD-box helicases are often associated with stress granules or P-bodies (processing bodies) (Beckham and Parker, 2008; Beckham *et al*., 2008; Buchan and Parker, 2009). Stress granules stabilize specific subsets of mRNA molecules, and prevent them from entering mRNA degradation pathways (Anderson and Kedersha, 2009; Balagopal and Parker, 2009; Buchan and Parker, 2009). The first step in degradation of mRNA is the shortening of the poly-A tail (deadenylation) followed by removal of the 5′ cap structure (decapping) (Beckham and Parker, 2008; Buchan *et al*., 2008; Anderson and Kedersha, 2009). Two proteins important to the stabilization of repressed transcripts in stress granules are the poly (A)- binding protein and the eukaryotic translation initiation factor 4 E (eIF4E), which binds the 5′ cap structure and prevents decapping (Balagopal and Parker, 2009; Buchan and Parker, 2009). In a recent study, protein components of the mRNP complexes that harbour DOZI interactions in female gametocytes were identified, and two of those proteins were in fact the poly (A)- binding protein and eIF4E (Mair *et al*., 2010).

Another recent study demonstrated that a kinase (IK2) that regulates the translation elongation factor eIF2-alpha provides a mechanism to maintain the salivary gland sporozoite in a translationally latent state (Zhang *et al*., 2010). Whereas disruption of SAP1 negatively affects the transcript abundance of a subset of genes found in salivary gland sporozoites, the disruption of the IK2 kinase lead to the premature translation of normally latent transcripts, including *UIS4*. Therefore, these two independent systems appear to use different means to control an important process: the silencing and maintenance of the infectivity of the mature salivary gland sporozoite as it waits to be injected into the vertebrate host.

As important differences have been reported on the localization of the *P. yoelii* and *P. berghei* orthologues of SAP1, we set out to resolve this apparent discrepancy through three independent methods (Aly *et al*., 2008; Silvie *et al*., 2008). First, through immunofluorescence microscopy using an antibody raised to the N-terminal domain of PySAP1, we observed a cytoplasmic staining pattern as we did previously with another SAP1-specific antibody to the C-terminus (Aly *et al*., 2008). Moreover, the speckled/granular staining pattern that we report for PySAP1 could be indicative of its localization to stress granules/P-bodies. Similar structures were also observed in salivary gland sporozoites by Zhang and colleagues (Zhang *et al*., 2010). Second, we attempted the fusion of PySAP1 with the fluorescent mCherry protein as was

done previously with the *P. berghei* orthologue (Silvie *et al.*, 2008). We were able to observe correctly transcribed and spliced mRNA products for this gene fusion in transgenic parasites, but could not detect the translated protein. Importantly, the phenotype of this parasite line resembled that of the *Pysap1*$^-$ parasites, as it failed to progress through liver stage development. This indicates that modification of the C-terminus of PySAP1 might destabilize the protein product, prevent its efficient translation, or both. It is feasible that in the instance of the *P. berghei* orthologue, the fusion of mCherry to its C-terminus may significantly and adversely affect its function and/or trafficking, leading to erroneous nuclear localization. Finally, we now present evidence that SAP1 has a role in post-transcriptional regulation of gene expression, through stabilization of a specific subset of sporozoite transcripts. Indeed, post-transcriptional regulation of gene expression is thought to be entirely a cytoplasmic process (Anderson and Kedersha, 2009; Balagopal and Parker, 2009; Buchan and Parker, 2009), in accordance with where we observe PySAP1 residing in sporozoites.

Significant differences have also been reported for *P. yoelii* and *P. berghei* in the effectiveness of using *sap1*$^-$ genetically attenuated parasites in vaccination. The study by Silvie and colleagues showed that *P. berghei sap1*$^-$ immunizations of C57BL/6 mice did not yield complete protection when immunized mice were challenged after 3 months pi (Silvie *et al.*, 2008). However, we show here in the *P. yoelii*/BALB/c model that complete long-lasting protection for up to 1 year is attainable with *Pysap1*$^-$ sporozoite immunizations. Importantly, we show that *Pysap1*$^-$ completely protects outbred mice, further demonstrating its potency as an immunogen. It will be of interest to test whether *P. berghei sap1*$^-$ immunizations are equally effective in outbred mice. One explanation for the difference in protection with *P. berghei* and *P. yoelii* might lie in their distinct infectivity for mice. BALB/c mice are substantially more susceptible to *P. yoelii* sporozoites than *P. berghei* sporozoites (Khan and Vanderberg, 1991). It is also known that *P. berghei* sporozoites are more promiscuous in their host cell preference and behave differently than sporozoites of other *Plasmodium* species (Hollingdale *et al.*, 1981; Silvie *et al.*, 2007). *P. berghei* also appears to target non-hepatocytic cells for infection and development, but it is currently unknown what consequences this has for the immunological host response (Gueirard *et al.*, 2010). Thus it might be possible that the effective vaccination dose and total amount of antigen with a given number of attenuated sporozoites is much higher in *P. yoelii* than in *P. berghei*.

Interestingly, *Pysap1*$^-$ immunizations are effective despite having greatly reduced transcript abundance for many sporozoite-expressed genes. Consequently, the proteins translated from these mRNAs are not necessary for inducing protection. *Pysap1*$^-$ sporozoites invade hepatocytes within a parasitophorous vacuole but then are deficient in early liver stage development (Aly *et al.*, 2008). This might indicate that many protective proteins are expressed during or shortly after infection.

The complete attenuation of liver stage development in *Pysap1*$^-$ parasites (i.e. no breakthrough infections) is likely due to the combined lack of a number of sporozoite proteins important for early LS development, such as UIS3 and UIS4. Interestingly, a considerable number of genes with transcripts that are downregulated in *Pysap1*$^-$ sporozoites encode for proteins that are predicted to be secreted or anchored in membranes such as the parasitophorous vacuole membrane. Thus, these proteins may directly interact with the host hepatocyte, and might be essential for early liver stage development and their analysis will give further insight into host–parasite interactions in the liver.

Experimental procedures

Experimental animals and parasites

Six-to-eight weeks old female BALB/c mice from the Jackson laboratory (Bar Harbor, ME) or Swiss Webster (SW) mice from Harlan (Indianapolis, IN) were used for immunizations or for parasite life cycle maintenance. Animal handling was conducted according to Institutional Animal Care and Use Committee approved protocols. *P. yoelii* 17 XNL (a non-lethal strain) wild-type and *Pysap1*$^-$ parasites were cycled between SW mice and *Anopheles stephensi* mosquitoes. Infected mosquitoes were maintained on sugar water at 24°C and 70% humidity. Salivary gland sporozoites were extracted from infected mosquitoes at day 15 post infected-blood meal. First, mosquitoes were rinsed in 70% ethanol then washed and dissected in RPMI medium. Collected mosquito tissues were ground gently with a tissue homogenizer, centrifuged at 800 r.p.m. for 3 min to remove mosquito debris and sporozoites were counted in a haemocytometer.

Sporozoite immunizations

For immunization and challenge studies, BALB/c or Swiss Webster mice were intravenously (iv) or subcutaneously injected with sporozoites resuspended in RPMI medium. Blood stage patency was monitored as previously described (Aly *et al.*, 2010). Each immunization group had an age-matched naïve control group (minimum three mice) that all became patent at day 3 after challenge with wild-type *P. yoelii* sporozoites.

Microarray construction

Plasmodium yoelii microarrays were produced in the Molecular Genomics Core Facility, Drexel University College of

Medicine. Each spotted array is composed of a 65-mer oligonucleotide microarray representing 6700 ORFs in the genome of the rodent malaria parasite *P. yoelii* (Carlton *et al.*, 2002).

RNA extraction and T7 RNA amplification

Wild-type and *Pysap1*$^-$ sporozoites were dissected at day 15 post blood meal and were purified over a DEAE cellulose column to remove contaminating mosquito tissue as previously described (Mack *et al.*, 1978). We used two independent biological replicates (each replicate with 5×10^6 sporozoites) for each genotype.

Total RNA was extracted from purified sporozoites using the Trizol reagent (Invitrogen). All samples were digested with *DNaseI* as prescribed by the manufacturer (Invitrogen). Total RNA was then subjected to two rounds of linear amplification using T7-based *in vitro* transcription according to manufacturer's protocol (Amino Allyl Message Amp II aRNA Amplification Kit, Ambion). Quality of total and amplified RNAs was examined with a high-resolution Agilent 2100 Bioanalyzer electrophoresis system (Agilent Technologies).

Target labelling and microarray hybridization

For microarray hybridizations, 10 μg of 2 × amplified RNA (aRNA) from each sporozoite population was coupled with Cy3 or Cy5 (Amersham). The procedure of the dye-coupling reaction and dye-labelled aRNA purification was followed according to the manufacturer's protocol (Amino Allyl MessageAmp II aRNA amplification kit, Ambion). The labelled aRNA was fragmented with Ambion's RNA fragmentation reagents for this procedure. The amount of aRNA used for hybridization was 5 μg per microarray. The differentially labelled RNA samples were mixed with 1.6 μl of 5 μg μl^{-1} yeast tRNA, 16 μl of 10 μg μl^{-1} poly(A) RNA, 9 μl SSC (20×) (1× SSC is 0.15 M NaCl plus 0.015 M sodium citrate), 0.6 μl sodium dodecyl phosphate (20%) and 1.2 μl HEPES (1 M). The hybridization mix was kept at 95°C for 2 min, 42°C for 20 min and 25°C for 5 min before being added to the microarray. Samples were applied beneath coverslips onto microarray slides. Dual hybridizations in duplicate with both orientations of dye incorporation (dye swaps) were performed in a 60°C water bath for 16 h under a lifter coverslip (Fisher) in hybridization chambers (Corning). The end wells were filled with 20 μl 3× SSC. Microarrays were removed from the hybridization chambers and washed in 1× SSC plus 0.1% sodium dodecyl phosphate for 2 min at room temperature, 0.2× SSC for 2 min, 0.05× SSC twice for 1 min and 0.01× SSC for 30 s. Slides were dried by centrifugation for 5 min at 60 *g*.

Microarray data analysis

Following hybridization and washing, the slides were scanned using a GenePix 4000A laser scanner and the array features (spots) were quantified using the GenePix Pro software program (Axon Instruments). Array data were analysed using the R statistical language and environment (http://www.r-project.org), specifically with the software packages from the Bio-conductor Project (http://www.bioconductor.org/). To survey the total number of genes detected in sporozoite populations, the feature intensities were first locally background corrected and then divided by the median intensity of negative control spots of the same channels on the same array. The negative controls were spotted with a single oligonucleotide of random sequence. The geometric mean of ratios was calculated for each oligonucleotide signal in each sample across all replicates. To detect differentially expressed genes, data were background corrected and then normalized using the VSN software package, which applies variance-stabilizing transformation (Huber *et al.*, 2002). Differentially expressed genes were then detected using the RankProd software package (Hong *et al.*, 2006) at a false-discovery rate of < 5%. The complete microarray data set can be accessed from the NCBI GEO database (Accession GSE12397).

Annotations

Protein domain annotations were done locally using Pfam (Bateman *et al.*, 2004), using pfam_scan.pl and by manual inspection of individual entries in PlasmoDB version 7.0 (Aurrecoechea *et al.*, 2009). Signal peptides were predicted using the SignalP 3.0 server (Bendtsen *et al.*, 2004). Only ORFs with a start codon were considered. Transmembrane domains were predicted using the TMHMM server, v. 2.0 (Krogh *et al.*, 2001). A gene was considered 'hypothetical' if the keyword 'hypothetical' appeared in its description line. *Plasmodium falciparum* orthologues were identified as reciprocal BLAST best hits as described in detail elsewhere (Tarun *et al.*, 2008). We annotated *P. yoelii* genes using the gene ontology annotations on their *P. falciparum* orthologues. *P. falciparum* gene ontology annotation was downloaded from the Gene Ontology Consortium website (http://www.geneontology.org).

Generation of antisera against N-terminus of SAP1

We generated rabbit polyclonal antiserum against the recombinantly expressed N-terminal domain of *Py*SAP1 (amino acids 2–233). Briefly the N-terminal domain of *Py*SAP1 was cloned into pET-28b(+) vector (Novagen), expressed as a 6 × His-fusion protein, and purified from the soluble protein fraction. The purified protein was used for rabbit immunizations (Pocono Rabbit Farm and Laboratories, PA), the final bleeds were collected, and the rabbit-specific IgGs were affinity purified on protein-G columns.

3′ and 5′ RACE analysis

Total RNA was extracted from both purified wild-type and *Pysap1*$^-$ sporozoites using the Trizol reagent (Invitrogen). All samples were digested with *DNaseI* (Invitrogen). Total RNA was then subjected to 3′ and 5′ RACE analysis according to instructions of the manufacturer (First Choice RLM-RACE, Ambion). For the 3′ RACE analysis, we isolated RNA and reverse transcribed it into cDNA using a oligo-dT attached to an upstream, base unbiased, DNA sequence (the 3′ DNA adaptor). The oligo-dT will bind selectively to the poly (A) tail of non-degraded transcripts. A combination of primers designed to amplify a fragment between the DNA adaptor

and a gene-specific 3′ UTR sequence will be only possible if the poly (A) tail is still present and not degraded. For the 5′RACE analysis, RNA isolated from *Pysap1*$^{-}$ and wild-type sporozoites was first phosphatase-treated to prevent the inclusion of uncapped transcripts in the subsequent analysis. Capped mRNA was then treated with the TAP (Tobacco Acid Pyrophosphatase) enzyme (+TAP) to remove the 5′ cap and expose a reactive phosphate group that can be ligated to a RNA adaptor of known sequence. Random decamers were then used to reverse transcribe the selected mRNAs to generate cDNA. Primer sets specific to the 5′ RNA adaptor sequence and gene-specific 5′ UTR sequences (5′ RACE test fragment) were used to selectively amplify sequences from the initially capped mRNAs. The sequences of the gene-specific primers are listed in Table S2.

Acknowledgements

This work was supported by the Bill and Melinda Gates Foundation through the Foundation at the National Institutes of Health Grand Challenges in Global Health Initiative. We would like to thank Dr Ashley Vaughan for critically reading this manuscript.

References

Aly, A.S., Mikolajczak, S.A., Rivera, H.S., Camargo, N., Jacobs-Lorena, V., Labaied, M., *et al.* (2008) Targeted deletion of SAP1 abolishes the expression of infectivity factors necessary for successful malaria parasite liver infection. *Mol Microbiol* **69:** 152–163.

Aly, A.S., Vaughan, A.M., and Kappe, S.H. (2009) Malaria parasite development in the mosquito and infection of the mammalian host. *Annu Rev Microbiol* **63:** 195–221.

Aly, A.S., Downie, M.J., Mamoun, C.B., and Kappe, S.H. (2010) Subpatent infection with nucleoside transporter 1-deficient *Plasmodium* blood stage parasites confers sterile protection against lethal malaria in mice. *Cell Microbiol* **12:** 930–938.

Anderson, P., and Kedersha, N. (2009) RNA granules: post-transcriptional and epigenetic modulators of gene expression. *Nat Rev Mol Cell Biol* **10:** 430–436.

Aurrecoechea, C., Brestelli, J., Brunk, B.P., Dommer, J., Fischer, S., Gajria, B., *et al.* (2009) PlasmoDB: a functional genomic database for malaria parasites. *Nucleic Acids Res* **37:** D539–D543.

Balagopal, V., and Parker, R. (2009) Polysomes, P bodies and stress granules: states and fates of eukaryotic mRNAs. *Curr Opin Cell Biol* **21:** 403–408.

Bateman, A., Coin, L., Durbin, R., Finn, R.D., Hollich, V., Griffiths-Jones, S., *et al.* (2004) The Pfam protein families database. *Nucleic Acids Res* **32:** D138–D141.

Beckham, C., Hilliker, A., Cziko, A.M., Noueiry, A., Ramaswami, M., and Parker, R. (2008) The DEAD-box RNA helicase Ded1p affects and accumulates in Saccharomyces cerevisiae P-bodies. *Mol Biol Cell* **19:** 984–993.

Beckham, C.J., and Parker, R. (2008) P bodies, stress granules, and viral life cycles. *Cell Host Microbe* **3:** 206–212.

Bendtsen, J.D., Nielsen, H., von Heijne, G., and Brunak, S. (2004) Improved prediction of signal peptides: signalP 3.0. *J Mol Biol* **340:** 783–795.

Buchan, J.R., and Parker, R. (2009) Eukaryotic stress granules: the ins and outs of translation. *Mol Cell* **36:** 932–941.

Buchan, J.R., Muhlrad, D., and Parker, R. (2008) P bodies promote stress granule assembly in Saccharomyces cerevisiae. *J Cell Biol* **183:** 441–455.

Carlton, J.M., Angiuoli, S.V., Suh, B.B., Kooij, T.W., Pertea, M., Silva, J.C., *et al.* (2002) Genome sequence and comparative analysis of the model rodent malaria parasite *Plasmodium yoelii yoelii*. *Nature* **419:** 512–519.

van Dijk, M.R., Douradinha, B., Franke-Fayard, B., Heussler, V., van Dooren, M.W., van Schaijk, B., *et al.* (2005) Genetically attenuated, P36p-deficient malarial sporozoites induce protective immunity and apoptosis of infected liver cells. *Proc Natl Acad Sci USA* **102:** 12194–12199.

Gueirard, P., Tavares, J., Thiberge, S., Bernex, F., Ishino, T., Milon, G., *et al.* (2010) Development of the malaria parasite in the skin of the mammalian host. *Proc Natl Acad Sci USA* **107:** 18640–18645.

Hollingdale, M.R., Leef, J.L., McCullough, M., and Beaudoin, R.L. (1981) In vitro cultivation of the exoerythrocytic stage of *Plasmodium berghei* from sporozoites. *Science* **213:** 1021–1022.

Hong, F., Breitling, R., McEntee, C.W., Wittner, B.S., Nemhauser, J.L., and Chory, J. (2006) RankProd: a bioconductor package for detecting differentially expressed genes in meta-analysis. *Bioinformatics* **22:** 2825–2827.

Huber, W., von Heydebreck, A., Sultmann, H., Poustka, A., and Vingron, M. (2002) Variance stabilization applied to microarray data calibration and to the quantification of differential expression. *Bioinformatics* **18** (Suppl. 1)**:** S96–104.

Kappe, S.H., Vaughan, A.M., Boddey, J.A., and Cowman, A.F. (2010) That was then but this is now: malaria research in the time of an eradication agenda. *Science* **328:** 862–866.

Khan, Z.M., and Vanderberg, J.P. (1991) Role of host cellular response in differential susceptibility of nonimmunized BALB/c mice to *Plasmodium berghei* and *Plasmodium yoelii* sporozoites. *Infect Immun* **59:** 2529–2534.

Krogh, A., Larsson, B., von Heijne, G., and Sonnhammer, E.L. (2001) Predicting transmembrane protein topology with a hidden Markov model: application to complete genomes. *J Mol Biol* **305:** 567–580.

Labaied, M., Harupa, A., Dumpit, R.F., Coppens, I., Mikolajczak, S.A., and Kappe, S.H. (2007) *Plasmodium yoelii* sporozoites with simultaneous deletion of P52 and P36 are completely attenuated and confer sterile immunity against infection. *Infect Immun* **75:** 3758–3768.

Le Roch, K.G., Johnson, J.R., Florens, L., Zhou, Y., Santrosyan, A., Grainger, M., *et al.* (2004) Global analysis of transcript and protein levels across the *Plasmodium falciparum* life cycle. *Genome Res* **14:** 2308–2318.

Mack, S.R., Vanderberg, J.P., and Nawrot, R. (1978) Column separation of *Plasmodium berghei* sporozoites. *J Parasitol* **64:** 166–168.

Mair, G.R., Braks, J.A., Garver, L.S., Wiegant, J.C., Hall, N., Dirks, R.W., *et al.* (2006) Regulation of sexual development of *Plasmodium* by translational repression. *Science* **313:** 667–669.

Mair, G.R., Lasonder, E., Garver, L.S., Franke-Fayard, B.M., Carret, C.K., Wiegant, J.C., *et al.* (2010) Universal features of post-transcriptional gene regulation are critical for *Plasmodium* zygote development. *PLoS Pathog* **6:** e1000767.

Matuschewski, K., Ross, J., Brown, S.M., Kaiser, K., Nussenzweig, V., and Kappe, S.H. (2002) Infectivity-associated changes in the transcriptional repertoire of the malaria parasite sporozoite stage. *J Biol Chem* **277:** 41948–41953.

Miao, J., Li, J., Fan, Q., Li, X., and Cui, L. (2010) The Puf-family RNA-binding protein PfPuf2 regulates sexual development and sex differentiation in the malaria parasite *Plasmodium falciparum*. *J Cell Sci* **123:** 1039–1049.

Mikolajczak, S.A., Silva-Rivera, H., Peng, X., Tarun, A.S., Camargo, N., Jacobs-Lorena, V., *et al.* (2008) Distinct malaria parasite sporozoites reveal transcriptional changes that cause differential tissue infection competence in the mosquito vector and mammalian host. *Mol Cell Biol* **28:** 6196–6207.

Mueller, A.K., Camargo, N., Kaiser, K., Andorfer, C., Frevert, U., Matuschewski, K., and Kappe, S.H. (2005a) *Plasmodium* liver stage developmental arrest by depletion of a protein at the parasite-host interface. *Proc Natl Acad Sci USA* **102:** 3022–3027.

Mueller, A.K., Labaied, M., Kappe, S.H., and Matuschewski, K. (2005b) Genetically modified *Plasmodium* parasites as a protective experimental malaria vaccine. *Nature* **433:** 164–167.

Shock, J.L., Fischer, K.F., and DeRisi, J.L. (2007) Whole-genome analysis of mRNA decay in *Plasmodium falciparum* reveals a global lengthening of mRNA half-life during the intra-erythrocytic development cycle. *Genome Biol* **8:** R134.

Silvie, O., Franetich, J.F., Boucheix, C., Rubinstein, E., and Mazier, D. (2007) Alternative invasion pathways for *Plasmodium berghei* sporozoites. *Int J Parasitol* **37:** 173–182.

Silvie, O., Goetz, K., and Matuschewski, K. (2008) A sporozoite asparagine-rich protein controls initiation of *Plasmodium* liver stage development. *PLoS Pathog* **4:** e1000086.

Tarun, A.S., Dumpit, R.F., Camargo, N., Labaied, M., Liu, P., Takagi, A., *et al.* (2007) Protracted sterile protection with *Plasmodium yoelii* pre-erythrocytic genetically attenuated parasite malaria vaccines is independent of significant liver-stage persistence and is mediated by CD8+ T cells. *J Infect Dis* **196:** 608–616.

Tarun, A.S., Peng, X., Dumpit, R.F., Ogata, Y., Silva-Rivera, H., Camargo, N., *et al.* (2008) A combined transcriptome and proteome survey of malaria parasite liver stages. *Proc Natl Acad Sci USA* **105:** 305–310.

Vaughan, A.M., Wang, R., and Kappe, S.H. (2010) Genetically engineered, attenuated whole-cell vaccine approaches for malaria. *Hum Vaccin* **6:** 107–113.

Zhang, M., Fennell, C., Ranford-Cartwright, L., Sakthivel, R., Gueirard, P., Meister, S., *et al.* (2010) The *Plasmodium* eukaryotic initiation factor-2alpha kinase IK2 controls the latency of sporozoites in the mosquito salivary glands. *J Exp Med* **207:** 1465–1474.

Supporting information

Additional supporting information may be found in the online version of this article.

Please note: Wiley-Blackwell are not responsible for the content or functionality of any supporting materials supplied by the authors. Any queries (other than missing material) should be directed to the corresponding author for the article.